

ROLE OF LAMB WAVE AND ATMOSPHERIC GRAVITY WAVE FOR THE 2022 HUNGA TONGA-HUNGA HA'APAI METEOTSUNAMIS

Ai Nishino, Kansai University, k069466@kansai-u.ac.jp
Takuya Miyashita, Kyoto University, miyashita.takuya.4w@kyoto-u.ac.jp
Tomohiro Yasuda, Kansai University, yasuda-t@kansai-u.ac.jp
Tomoya Shimura, Kyoto University, shimura.tomoya.2v@kyoto-u.ac.jp
Nobuhito Mori, Kyoto University, mori@oceanwave.jp

1. BACKGROUND

On January 15, 2022, a massive eruption occurred at the Hunga Tonga-Hunga Ha'apai volcano in the Tonga islands, South Pacific Ocean. The eruption resulted in rapid atmospheric pressure changes and tsunamis along the Pacific coast. Along the coast of Japan, tsunami waves were observed several hours earlier than the expected arrival time due to the pressure change of about 2 hPa, and the subsequent tsunami heights exceeded 1 m at several tide stations. These surface fluctuations were categorized as meteotsunamis, in which the sea surface is excited by atmospheric pressure. Proudman resonance and bay oscillations were assumed to contribute to the amplification, but the factors which caused the large amplification off the coast of Japan are not clarified. This study aims to estimate the primary factors of the maximum tsunami amplitude in Japan by comparing numerical simulations under multiple atmospheric pressure wave conditions with the observation records by Japan Meteorological Agency (JMA) and Ports and Harbours Bureau, MLIT.

2. METHODOLOGY

(1) Creation of atmospheric external force data

Atmospheric pressure conditions due to the volcanic eruption were created using climate parameters based on observation records and previous studies. Figure 1 shows the observed and assumed spatio-temporal data of pressure waves (atmospheric Lamb waves and atmospheric gravity waves) and their wavelet analysis results. For the Lamb wave, the velocity was assumed to be 310 m/s based on observation records, and the amplitude was determined to be about 2 hPa around Japan as a function of distance from the volcano concerning the parameters of Gusman et al.[1] Atmospheric gravity waves were assumed to reproduce the observed pressure waveforms by superimposing a finite number of waves of various wavelengths, considering dispersion relations. In total, three pressure patterns were created. Pres. L indicates the case where only Lamb waves propagate, whereas Pres. A and B include air gravity waves. Pres. A was intended to match the observed waveforms. Pres. B has longer periods of pressure oscillation. In addition, atmospheric gravity waves in Pres. B propagate continuously to reproduce the resonance in the bay.

(2) Tsunami simulation

Numerical tsunami simulations were performed using the sea surface pressure created as shown in Figure 1. The numerical model GeoClaw, which solves nonlinear shallow water equations, was used for tsunami simulations. GeoClaw incorporates the adaptive mesh refinement (AMR), which is a method that dynamically

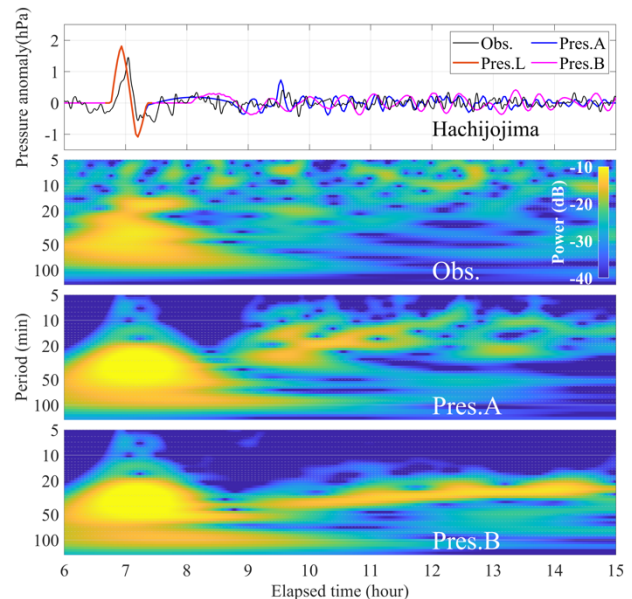


Figure.1 Time series of pressure waveform and wavelet analysis at Hachijojima pressure gauge, in the Izu Islands south of Tokyo, Japan. The top figure shows a comparison between the created and observation waveforms. The other figures show the result of wavelet analysis result for observed data and Pres A, B, and C.

changes the spatial resolution and time interval during the computation. Five resolution levels were set: 12 arcminutes, 4 arcminutes, 1 arcminute, 15 arcseconds, and 5 arcseconds. The simulation domain was set to latitude 55°N to 55°S and longitude 115°W to 200°E, including the North Atlantic region. The computed time is 15 hours from the eruption.

RESULTS AND DISCUSSION

Figure 2 shows the comparison between the results of the tsunami simulation considering the Lamb wave and atmospheric gravity waves with the waveforms observed at Chichijima (in Ogasawara islands) and Kuji (in Tohoku). The blue and pink lines show the calculation results for the Pres A and Pres B conditions, and the dotted and solid lines show the simulated results for a maximum of 1 arcminute and 5 arcseconds. Hereafter, simulations at 1 arcminute and 5 arcseconds are referred to as low and high resolutions, respectively. The first tsunami wave under the Pres L condition (orange line), in which only Lamb waves were considered, generally coincides with the observed initial tsunami around arrival time. In addition, the waveform simulated well for about 2 hours after the initial tsunami arrival. These results indicate that the initial water

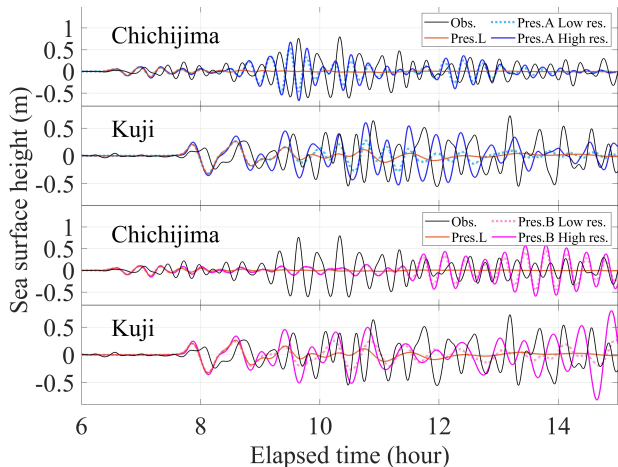


Figure.2 Comparison between simulated result and observed tsunami waveforms at tide gauges (Chichijima and Kuji). Black lines indicate observed waveforms. Dotted and solid lines indicate simulated waveforms for Low res. and High res.

level change was excited by the Lamb wave, and the effect lasted for about 2 hours.

Figure 3 shows the spatial distribution of the maximum amplitude under PresA conditions from 0 to 15 hours after the eruption. The figure shows that amplification occurs more along the Pacific coast than offshore due to the propagation of pressure waves. As shown in Figure 2, the simulated waveform with low resolution under Pres A (dotted line) at Chichijima reproduces the observed waveforms well. In contrast, at Kuji, the simulated amplitude was only about 20 cm, and the maximum amplitude was not reproduced. However, the simulated waveform at Kuji with high-resolution (solid line) shows good agreement with the observed one. This indicates that the waveforms are significantly amplified in coastal areas, not in the offshore. Thus, the contribution of Proudman resonance was minor at this site. Similar results were obtained not only in Kuji but also at several ports in eastern Japan.

Figure 4 shows a summary of the comparison of simulated and observed maximum amplitudes under Pres B conditions. The simulated results correspond to the observation relatively in the Okinawa region, located in southwestern Japan and along the eastern coast of Japan. The high-resolution calculation results show significant amplification along the Tohoku coasts. This result suggests that the maximum amplitudes at these locations were caused by the weak incident waves with resonant components for a long duration. However, in Amami and Shikoku regions on the western coast of Japan, there was a large difference between the observed and simulated maximum amplitudes. Reproducing tsunami amplification at these locations is challenging, and other mechanisms than bay resonance and Proudman resonance can contribute to the amplification.

CONCLUSIONS

The results of tsunami simulation of the Tonga volcanic eruption showed that the waveforms and maximum amplitude along the east coast of Japan were well

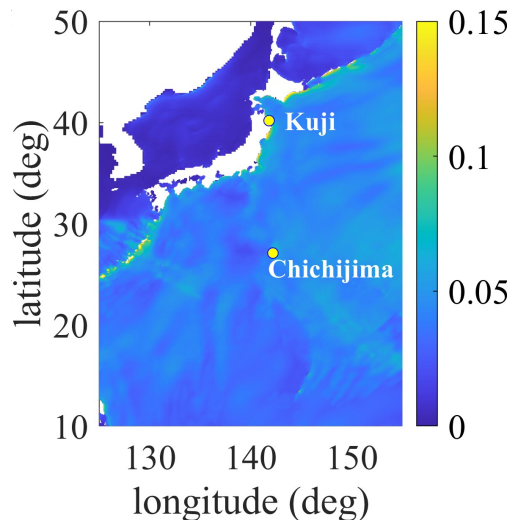


Figure.3 Spatial distribution of simulated maximum amplitudes around Japan by PresA condition.

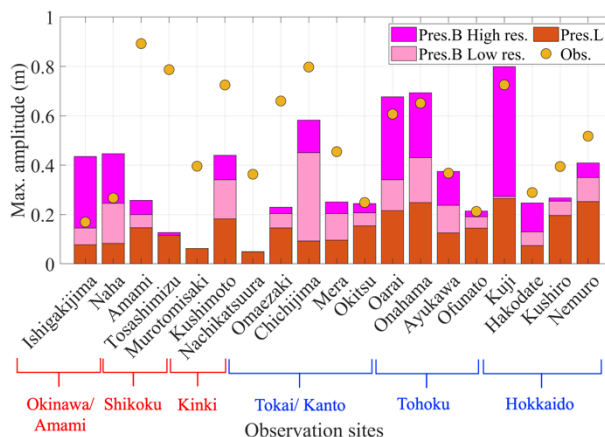


Figure.4 Comparison of observed and simulated maximum amplitudes. The observation sites are arranged in order from western Japan from the left. The maximum amplitudes under each condition are indicated by the color bar. Circles indicate observed amplitudes.

simulated. Especially along the Tohoku coast, the observed maximum amplitude cannot be explained by the velocity component causing Proudman resonance, and the harbor oscillations contribute relatively high. At stations with relatively small maximum amplitudes, shallow water deformation and Proudman resonance were estimated to be the main factors of the maximum amplitude. On the other hand, the maximum amplitude could not be simulated well for Amami and Shikoku. At these locations, specific frequency components, which are not largely included in the pressure waves, may be amplified in the ocean and contribute to the amplification of tsunami.

REFERENCES

[1] Gusman, A. R., Roger, J., Noble, C., Wang, X., Power, W., Burbidge, D. (2022): The 2022 Hunga Tonga-Hunga Ha'apai Volcano Air-Wave Generated Tsunami, *Pure and Applied Geophysics*, 179, pp.3511-3525.